Highly Fluorinated Poly(arylene alkylene ether sulfone)s: Synthesis and Thermal Properties†

Jianfu Ding,*,‡ Xiaomei Du,‡ Michael Day,‡ Jia Jiang,§ Claire L. Callender,§ and Jacek Stupak⊥

Institute for Chemical Process and Environmental Technology, National Research Council of Canada, 1200 Montreal Road, Ottawa, Ontario, Canada K1A 0R6; Communications Research Centre Canada, Ottawa, Ontario, Canada K2H 8S2; and Institute for Biological Sciences, National Research Council of Canada, 100 Sussex Drive, Ottawa, Ontario, Canada K1A 0R6

Received January 3, 2007; Revised Manuscript Received February 28, 2007

ABSTRACT: A simple procedure has been developed for the preparation of highly fluorinated poly(arylene alkylene ether sulfone)s using a nucleophilic polycondesation reaction of decafluorodiphenyl sulfone (DPSO) with a series of fluorinated linear or branched alkylene diols containing 4−12 carbon atoms. The reactions are activated using cesium fluoride (CsF) or potassium fluoride (KF) as a base in *N*,*N*-dimethylacetamide (DMAc) at room temperature and are completed in a few hours or a few days, respectively. Polymers with number-average molecular weights (M_n) around 50 000 Da have been prepared. A broad molecular weight distribution and a low dependence of the reaction rate on temperature are observed and attributed to the heterogeneous nature of the reactions. Because of low solubility, CsF and KF exist in the reaction solution mainly in the form of solid particles, and the adsorption of the polymer on the surface of the particles hinders the diffusion of CsF and KF from solid into solution. This effect causes the polymers close to the solid surface to have greater growth rates and higher molecular weights than those in solution. Polymers with linear alkylene spacers display a marked tendency to crystallize, which increases with the length of the alkylene spacer. In fact, the polymer with the longest alkylene spacers ($P12C_FSO$) crystallizes during the polymerization reaction, preventing the polymer chains from growing, resulting in a low molecular weight (M_n < 8000 Da). Raising the reaction temperature to 70 °C slightly decreases the crystallization tendency and allows the M_n to increase to 17 000 Da. The crystallization of $P12C_FSO$ is fast enough to be completed during a quenching process induced by immersing the molten sample in liquid nitrogen. However, the polymer with branched alkylene spacers does not show any crystalline structure even when annealed at a temperature slightly higher than its glass transition temperature (T_g). A secondary crystal peak is also found in the DSC curves of the crystalline polymers with linear alkylene spacers. The position of this peak can be shifted to higher temperatures by annealing and has been attributed to incomplete crystallites formed between the primary lamellar crystals.

Introduction

Highly fluorinated polymers have generated significant research interest recently due to attractive properties, including highly thermal and chemical stability, low surface energy, and low optical loss in the optical communication wavelength region (∼1550 nm). A wide variety of fluorinated polymers such as fluorinated polyacrylate, fluorinated polyimide, fluorinated poly(arylene ether)s, and poly(tetrafluoroethylene) (Teflon) have been developed for many applications.[1] However, most of the materials developed so far are only partially fluorinated materials with relatively low fluorine contents. Highly fluorinated polymers such as Teflon are difficult to process into high-quality films, thereby restricting their applicability. As a consequence, the innovative development of new types of highly fluorinated polymers with easy processability has become very attractive. Herein, we report the development of a series of novel highly fluorinated poly(arylene alkylene ether sulfone)s (PmC_FSO) prepared from the nucleophilic polycondensation reactions of decafluorodiphenyl sulfone (DPSO) with a series of fluorinated linear or branched alkylene diols (mC_F-diols, see Scheme 1).

Though great efforts have been made in exploring the preparation of the poly(arylene alkylene ether)s, successful examples are rare.[2−5] Among them, we believe the nucleophilic polycondensation reaction of a decafluorodiphenyl compound with a fluorinated alkylene diol to be the most promising. The difficulties in carrying out this reaction have been attributed to the hydroxyl group of the diol, which has much lower acidity in comparison with the phenol group of aromatic bisphenols used for the analogous reaction for the preparation of poly(arylene ether)s. Consequently, it is traditionally thought that a strong base (such as NaH) is required to convert the hydroxyl group into the alkoxide anion nucleophile for activating the reaction,[2,3] or alternatively the hydroxyl group has to be masked to promote the substitution reaction.[3,4] Unfortunately, we have found that the use of strong base results in side reactions and reduces the selectivity of the reaction at the para position of the perfluorodiphenyl monomers with the general structure

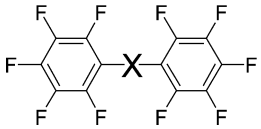

These side reactions result in branched and even cross-linked polymers and break the stoichiometric balance between para fluorines and OH groups, which is required in order to obtain high molecular weight polymers. As a result, from a series of

* Corresponding author: e-mail jianfu.ding@nrc-cnrc.gc.ca, phone (+613) 993-4456.

† NRC Publication No. 49115.

‡ Institute for Chemical Process and Environmental Technology, NRC.
§ Communications Research Centre Canada.
⊥ Institute for Biological Sciences, NRC.

10.1021/ma070013y CCC: $37.00 Published 2007 by the American Chemical Society
Published on Web 04/07/2007

Scheme 1. Preparation of the Highly Fluorinated Poly(arylene alkylene ether sulfone)s

R_f(m=4-12)	$-CH_2(CF_2)_{m-2}CH_2-$	$-CH_2CFCH_2-$ $(CF_2)_4$ F
Polymer	PmC_FSO	$P7_bC_FSO$

perfluorodiphenyl monomers, only the monomer with a single bond as the bridging X (i.e., perfluorobiphenyl) has been successfully polymerized to give high molecular weight polymers.[5] In this case, the polymerization benefits from the specific structure of perfluorobiphenyl, where the four ortho fluorines overlap due to the short distance between the adjacent phenyl rings to create significant steric hindrance for the reaction at these four ortho positions. When the bridging X becomes a longer unit such as a ketone group (i.e., decafluorobenzophenone), the side reactions at the ortho positions become more likely, and consequently only low molecular weight oligomers (M_n = 5200 Da) could be produced even when mild reaction conditions were employed.[5]

In our previous papers, we reported a simple and mild route for the synthesis of a series of highly fluorinated poly(arylene ethers) using CsF or KF as a base to activate hexafluorobisphenol A to react with a decafluorodiphenyl monomer such as decafluorobenzophenone, decafluorodiphenyl sulfone (DPSO), and decafluorodiphenyloxadiazole.[6] This base system has now been successfully adapted for activating a series of fluorinated alkylene diols to react with DPSO for the preparation of a series of highly fluorinated poly(arylene alkylene ether sulfone)s, as summarized in Scheme 1.

In this reaction scheme, mC_F represents a fluorinated alkylene spacer containing *m* carbons. In addition to the polymers with linear alkylene spacers, a polymer with a branched alkylene spacer ($P7_bC_FSO$) has also been prepared, where subscript b represents the branched structure. The introduction of the fluorinated alkylene spacers into the polymers instead of arylene spacers will result in materials with a reduced T_g, refractive index and surface energy, and a tunable crystallinity. In addition, it is shown that the reaction is clean and free of side reactions, leading to the production of polymers with well-defined structures and high molecular weights.

Results and Discussion

1. Polycondensation of DPSO with Fluorinated Diols. The polycondensation was conducted under mild reaction conditions in DMAc using CsF or KF as a base to convert the hydroxyl group to the alkoxide anion for activating the reaction with DPSO. As illustrated in Scheme 2, in the reaction, CsF or KF also combines with HF, which is produced from the reaction as a byproduct, to form a $CsHF_2$ or KHF_2 complex that precipitates out of the solution,[7−9] allowing the reaction to go to completion, generating a high molecular weight polymer.

This reaction has been monitored using ^{19}F NMR analysis. Figure 1 illustrates the results for the reaction of DPSO with $6C_F$-diol in the presence of KF. Five peaks are clearly evident in the ^{19}F NMR spectrum of the initial reaction solution (0.0 h) at −123.0, −124.9, −138.4, −145.0, and −161.1 ppm, which

Scheme 2. Reaction Scheme for the Formation of Ether Linkage Following S_NAr Mechanism

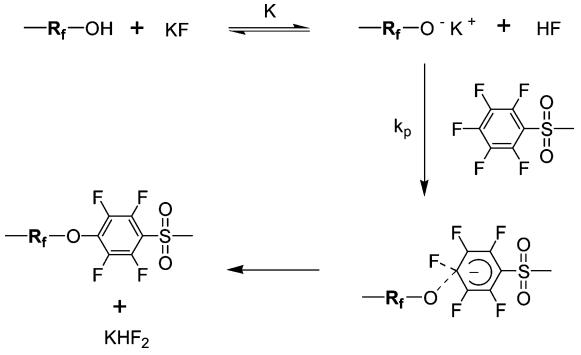

are attributed to the fluorine atoms on C-3 and C-4 (d′) and C-2 and C-5 (e′) of $6C_F$-diol and ortho (a′), para (c′), and meta (b′) fluorine atoms of DPSO, respectively. It can be seen that the peak associated with the para fluorines decreased in intensity and eventually disappeared completely, while the other peaks shifted to −121.8, −124.3, −140.0, and −155.7 ppm as the formation of the ether linkage progressed. In addition, some other peaks were also formed during the reaction but eventually

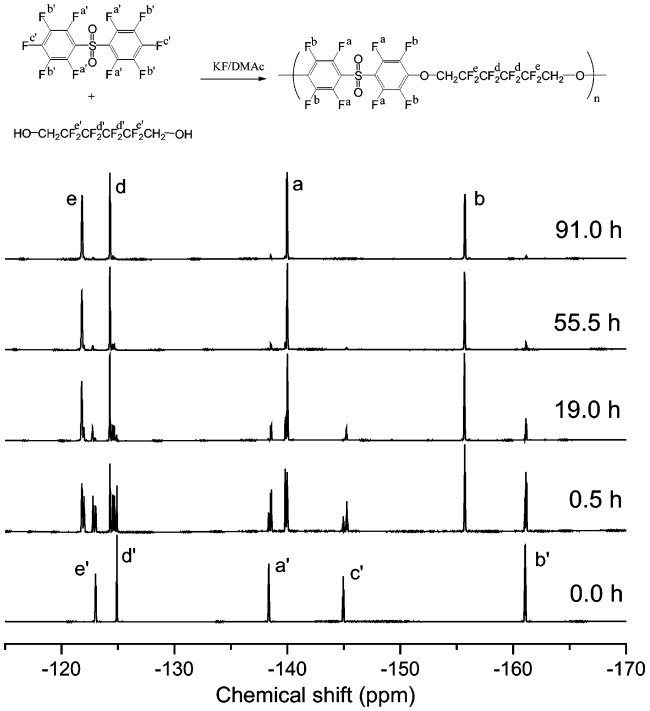

Figure 1. ^{19}F NMR spectra of the solution taken from the reaction of DPSO with C_F6-diol ([F]/[OH] = 1.005:1.000) in the presence of KF (1.5 equiv vs OH) in DMAc at 22 °C at 0.0, 0.5, 19.0, 55.5, and 91.0 h.

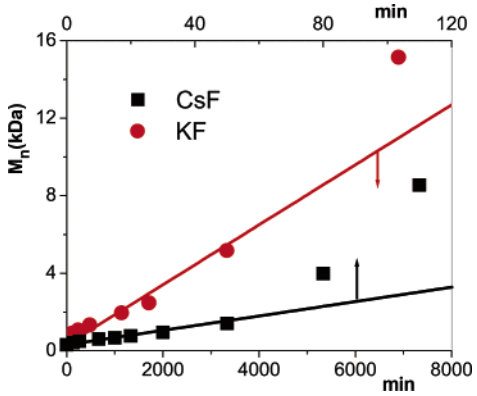

Figure 2. Variation of M_n with the reaction time of the polymers produced from the polycondensation of DPSO with C_F6-diol ([F]/[OH] = 1.005:1.000) in DMAc at 22 °C in the presence of KF (cycle) or CsF (square) (1.5 equiv vs OH). The solid lines are fits of the data to eq 3.

disappeared. They are related to the corresponding fluorine atoms on the end units in the resulting oligomers and polymers. By comparing the integral intensity of these peaks, the conversion ($p = ([F]_0 - [F]_t)/[F]_0$, where $[F]_0$ and $[F]_t$ are the para fluorine concentrations in the initial reaction solution and at time, t) at different reaction times can be calculated. The number-average molecular weight (M_n) of the resulting polymer can be further derived by considering the feed ratio of the monomers (r_0) using following equation[10]

$$M_n = \frac{M_0(1 + r_0)}{2r_0(1 - p) + (1 - r_0)} \quad (1)$$

where M_0 is the average molecular weight of the monomers. The calculated results are presented in Figure 2 as a function of the reaction time.

CsF was found to be very reactive for the polycondensation of DPSO with the fluorinated diols listed in Scheme 1. The reaction with 6C_F-diol was completed in 4 h to give a polymer with M_n = 44 000 Da. However, the reaction activated by KF exhibited a lower reaction rate and only resulted in a polymer with a high molecular weight (M_n = 30 600 Da) after 150 h. This reaction time is too long for an economical polymer synthesis. Consequently, only CsF was used for the preparation of the other polymers investigated in this study. The reaction conditions are summarized in Table 1. Under these reaction conditions, polymers with M_n around 50 000 Da and M_w/M_n values of 3.4−6.5 have been obtained. The exception to this trend was the polymer P12C_FSO, in which crystallization of the polymer during polymerization was noted (see below).

2. Effect of Crystallizing on the Polymerization. While the majority of the polymers obtained in this study had high molecular weights, the preparation of the polymer with the longest alkylene spacer, P12C_FSO, only produced a low molecular weight polymer with a M_n less than 8000 Da. It is very interesting to note that at the end of this reaction the solution becomes highly viscous. In fact, the viscosity was high enough to stop magnetic stirring even when the solution was diluted to about 4% of solid content. A further investigation revealed that a gel-like substance formed during the reaction. However, the isolated polymer from this solution was found to be soluble in boiling tetrahydrofuran (THF) and has a narrow molecular weight distribution ($M_w/M_n \sim 2.5$), indicating that the gel-like material is not associated with branched or cross-linked structures which could be produced by side reactions. Considering the extremely high crystallization tendency of this polymer (discussed later), we therefore believe that this gel-like structure is associated with the crystallization of the polymer chain in the solution. This effect prevents further growth of the polymer chain. In order to minimize the crystallization, alternative solvents and higher reaction temperatures were examined for the reaction. Among the tested solvents including DMAc, *N*,*N*-dimethylformamide (DMF), dimethyl sulfoxide (DMSO), *N*-methylpyrrolindinone (NMP), and propylene carbonate (PC), DMAc was found to give the best results. Conducting the reaction at a higher temperature (40 °C) in DMAc or NMP did not increase the molecular weight, but rather resulted in a molecular weight decrease after a prolonged reaction time. This was attributed to the degradation of the polymer, which was verified by the appearance of some unidentified peaks in the ^{19}F NMR spectra. Our previous work demonstrated that the use of CaH_2 along with a catalyzing amount of CsF could effectively activate the reaction and sufficiently suppress the side reaction associated with the degradation of fluorinated aromatic polyethers at high temperatures.[6d] Therefore, a mixture of CsF (0.5 equiv) and CaH_2 (2.0 equiv relative to OH group) was used as the base for this reaction conducted in DMAc at 70 °C. The reaction solution became very viscous and gel-like after 4 h. The final reaction mixture after 5 h was dropped into a methanol/H_2O (1/1) mixture to precipitate the polymer and dissolve the inorganic solids. After thoroughly washing with water and methanol, the white precipitate was measured by SEC and showed a M_n = 17 700 Da, which is about twice that of the polymer prepared at room temperature with CsF alone.

3. Reaction Kinetics. Following the aromatic nucleophilic substitution mechanism (S_NAr, see Scheme 2), this reaction was controlled by the formation of Meisenheimer complex intermediate.[11] Consequently, eq 2 can be derived for the polymerization with a perfect stoichiometry to describe the relationship of the conversion with the reaction time

$$\frac{1}{1 - p} = 1 + kC_0t \quad (2)$$

where p is the conversion at reaction time t, C_0 is the initial concentration of the monomers, and $k = Kk_p[K^+]/[HF]$ is the apparent reaction rate constant (see Scheme 2), where K is equilibrium constant for the formation of the alkoxide and k_p is the rate constant for the formation of the Meisenheimer complex. In this study, in order to produce high molecular weight polymers and avoid the side reaction at the ortho position of the decafluorodiphenyl monomer, r_0 close to, but always less than 1.00 ($r_0 = [OH]/[F] = 0.995$) was chosen. At this r_0 value, the second term in the denominator of eq 1 can be omitted to simplify the kinetics discussion. This approximation will cause an error less than 5% in M_n calculation when the conversion is less than 95%. After this approximation, eq 2 can be combined with eq 1 to yield the following linear relationship between M_n and reaction time.

$$M_n = \frac{M_0(1 + r_0)}{2r_0}(1 + kC_0t) \quad (3)$$

The experimental data presented in Figure 2 were found to fit this equation satisfactorily when the molecular weight is less than 5000 Da, confirming that the reaction follows the S_NAr mechanism.

4. Molecular Structures of the Polymer and Oligomers. The molecular weights of the polymers produced at different reaction times were also checked using SEC, and the results for the reaction of DPSO with 6C_F-diol in the presence of CsF

Table 1. Preparation and Characterizations of Polymers

polymer	time[a] (h)	M_n[b] (kDa)	M_w/M_n[b]	T_g[c] (°C)	T_m[d] (°C)	ΔH[d] (J/g)	$T_d^{5\%}$[e] (°C)
P4C_FSO	12.0	41.5	4.5	102.6	196.2	15.0	396.0
P5C_FSO	14.0	41.0	4.9	96.8	187.7	12.6	389.9
P6C_FSO	4.0	44.0	6.5	87.0	173.9	10.6	415.3
P8C_FSO	8.0	85.3	6.0	86.1	192.0	14.1	418.4
P10C_FSO	6.0	33.0	3.8	78.3	213	15.7	403.3
P12C_FSO	5.0[f]	17.7	3.1	n/a	227.5	26.0	398.8
P7$_b$$C_F$SO	8.0	12.2	3.4	94.7	n/a	n/a	401.2

[a] The polymerization was conducted in DMAc in the presence of CsF at 22 °C. [b] M_n and M_w/M_n values are PS equivalent obtained from SEC measurement. [c] T_g values were measured from the second heating scans of slowly cooled samples (cooled from 250 °C at 10 °C/min), while quenched samples (quenched from 250 °C into liquid nitrogen) were measured for the high crystalline polymers, P10C_FSO and P12C_FSO, in order to make the glass transition observable. [d] T_m and ΔH were recorded form the first heating scan of the DSC measurement. [e] $T_d^{5\%}$ was the degradation temperature at which 5% weight loss was detected in TGA measurement under the protection of nitrogen. [f] The reaction was activated by a mixture of CsF (0.5 equiv)/CaH_2 (2.0 equiv) in DMAc at 70 °C.

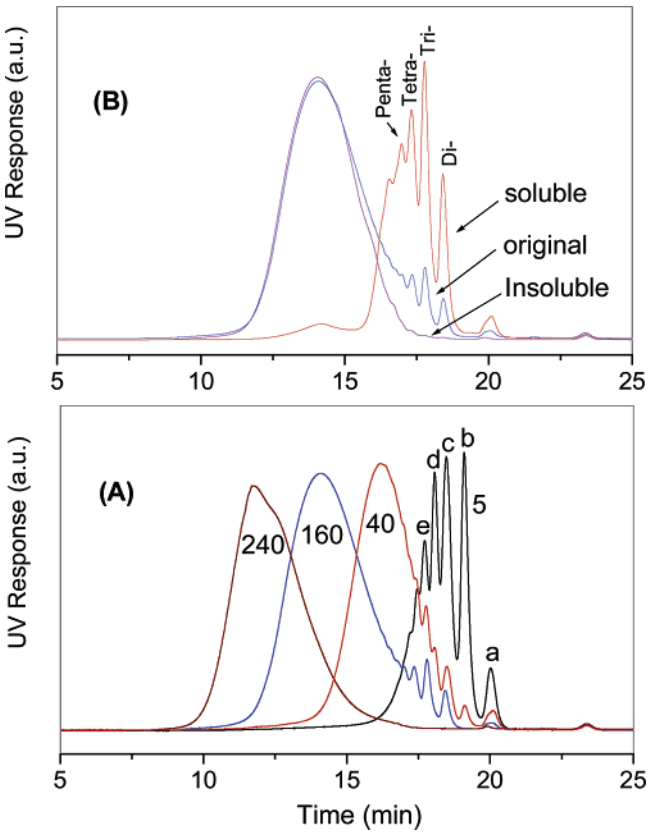

Figure 3. (A) SEC curves of the samples taken at 5, 40, 160, and 240 min from the reaction of DPSO with 6C_F-diol in the presence of CsF in DMAc at room temperature. The samples taken at 5, 40, and 160 min were obtained by precipitating the solution into a methanol/H_2O (1/1) mixture, while the sample taken at 240 min is precipitated into methanol. (B) SEC curves of the original sample and the fractions soluble and insoluble in an acetone/methanol (1/9, v/v) mixture of the samples taken at 160 min.

are displayed in Figure 3. In this experiment, the samples collected at 5, 40, and 160 min were precipitated into a methanol/H_2O (1/1 by volume) mixture to recover organic materials including high molecular weight polymer and low molecular weight oligomers. Meanwhile, the final sample (240 min) was precipitated twice in methanol, so that most of the low molecular weight materials were removed.

The SEC trace of the 5 min sample displays multiple peaks, which are apparently associated with the monomer and low molecular weight oligomers. By comparing with the SEC traces of the monomers, peak a is easily assigned to DPSO. The assignment of the other peaks in this SEC trace is difficult due to the overlap of the peaks associated with the different oligomers. However, some conclusions can be drawn by comparing the SEC traces of 5, 40, and 160 min samples. Peaks b and d completely disappeared after a long reaction time, while peaks c and e remained to some extent during the reaction, which would be consistent with the formation of the cyclic oligomers. Therefore, peaks c and e can be assigned to oligomers containing an even number of monomer units, from which cyclic oligomers are possibly formed, while peaks b and d are related to the oligomers consisting of an odd number of monomer units, which are not able to form cyclic structures due to their possession of identical end groups.

The formation of the cyclic oligomers is unavoidable during the polycondensation reaction. It has been demonstrated that the fraction of cycles could be more than that of linear polymers in some reactions when the stoichiometry is close to perfection.[12a,b] The formation of the cyclic fraction apparently broadens the molecular weight distributions of the resulting polymers. Figure 3B demonstrates the influence of the presence of the low molecular weight oligomers on the M_w/M_n value of the resulting polymer. For this purpose the original 160 min sample was purified by precipitating the 5% polymer solution in THF into acetone/methanol (1/9, v/v), and then the soluble fraction and the insoluble fraction were both checked using SEC. The SEC curve of the original 160 min sample results in an M_w/M_n value of 3.03. The purification completely removed the low molecular weight peaks from the SEC curve and narrowed the M_w/M_n value to 1.84. The soluble fraction counted for 11 wt % of the original sample, and its SEC curve in Figure 3B showed that this fraction mainly consisted of low molecular weight oligomers corresponding to a few narrow peaks. The peak molecular weights indicate that these peaks correspond to oligomers containing 2−5 repeat units. A MALDI-TOF mass spectrum of this sample in Figure 4A demonstrated that this low molecular weight fraction mainly consisted of cyclic oligomers containing 2−5 repeat units with the cyclic trimer having the highest intensity. Considering the low weight percentage of this fraction and the fact that the cyclic trimer is the dominant species of the cycles, we believe the cyclization is moderate and mainly occurred at low conversion under this reaction condition. This result can be attributed to the extremely mild condition used for this reaction, under which the side reactions which may cause cyclization, such as "backbiting" reactions can be avoided.[12c,d] This explanation can be further confirmed by the MALDI-TOF mass spectra (Figure 4B) of the sample taken from the reaction at 10 min, in which only one small peak associated with cycles, that of the cyclic trimer, can be identified with an intensity of about 3% of the corresponding linear oligomer.

It is worth noting that the SEC trace of the highest molecular weight sample in Figure 3 displays a bimodal peak, which gives a broad molecular weight distribution with a M_w/M_n value of 6.5 (M_n = 44 000 Da). This value is much higher than that of

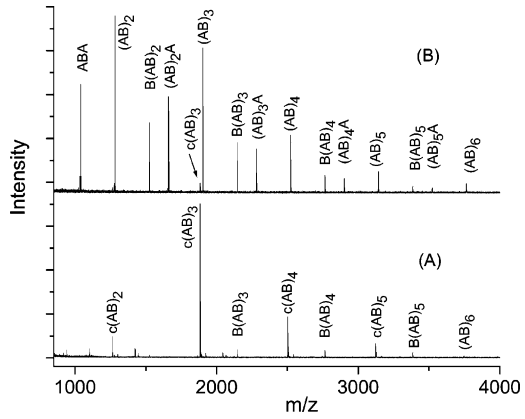

Figure 4. MALDI-TOF mass spectra of the samples taken at 10 min (B) and the soluble fraction (in 10/90 acetone/methanol) of the sample taken at 160 min (A) from the reaction of DPSO with $6C_F$-diol in the presence of CsF in DMAc at room temperature. Peaks correspond to $[M + Na]^+$ and were assigned using a combination of symbol A and B, where A represents DPSO unit and B represents $6C_F$-diol unit, and the prefix c means cyclic structure, while the others without the prefix are linear structures.

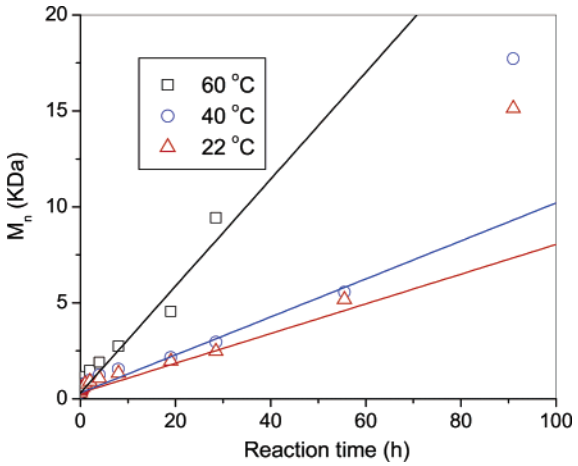

Figure 5. Variation of M_n with reaction time of the polymers produced from the polycondensation of DPSO with C_F6-diol ([F]/[OH] = 1.005:1.000) in DMAc in the presence of KF (1.5 equiv vs OH) at 22 (triangle), 40 (circle), and 60 °C (square). The solid lines are fits of the data to eq 3.

a typical polycondensation reaction (~2.0). It is surmised that this broad distribution is probably caused by the side reaction at the ortho positions of DPSO, which are usually found in the polycondensation between DPSO with bisphenols.[6e,13] The high causticity of the alkoxide anion leads to a high reactivity for the nucleophilic polycondensation reaction and may result in a reduced selectivity of the reaction at the para position of DPSO. However, the ^{19}F NMR study of this sample revealed a very clean spectrum, which is similar to that of the 91 h sample in Figure 1, indicating that the number of branching sites is much smaller than the number of end groups. Therefore, it is very unlikely that branching is the cause of the broad molecular weight distribution in this sample. Another possible explanation is the formation of the cyclic oligomers and polymers. Cyclization is unavoidable in the polycondensation reaction and could result in the M_w/M_n values gradually increasing up to 10 with the increase of the conversion.[12a] However, as indicated in the above discussion, the cyclization is not a major issue in this study due to the use of a mild reaction condition. The SEC results in Figure 3 also indicated that the purified polymer taken from the reaction at 160 min had a low M_w/M_n value (1.84). It is only in the last 80 min of the reaction that the M_w/M_n value rapidly increased from 1.84 to 6.5. During this reaction period, the molecular weight of the polymer is already high. Because CsF or KF exists in the solution mainly as solid particles due to low solubility, the high molecular weight polymer may become adsorbed on the solid surface to form a tough layer, preventing the efficient migration of both the base and the polymer chain from the solid surface to the solution. A higher concentration of the base near the solid surface would build up at this time. Therefore, polymers close to the solid surface will have a higher growth rate, leading to higher molecular weights than those attained by polymers more remote from the surface. In order to verify this assumption, polymers on the surface of the solid particles and in the solution were separated by centrifuging the reaction solution taken at 160 min. The polymer adsorbed on the solid sample was extracted by dissolving the inorganic solid in a methanol/H_2O (1/1) mixture. SEC analysis was then performed on the polymer obtained from the solution and the polymer extracted from the solid surface. The polymer from the solid surface displayed a broad peak with the peak position at 115 kDa, about 5 times higher than that of the polymer from the solution (23.9 kDa), and a M_w/M_n value of 6.2, about twice that from the solution (3.03). This difference is believed to be attributed to a higher growth rate of the polymer near the solid surface due to the higher concentration of base in this region. This observation also suggests that the exchange of the polymers between the surface and the solution is insufficient for a homogeneous product. Meanwhile, no insoluble gel was found in the sample extracted from the solid surface, confirming again that the branching side reaction is not an issue under this reaction condition. Hence, we can conclude that the heterogeneous reaction condition is the main cause of the broad molecular weight distribution.

5. Temperature Effect on the Reaction. Because the reaction in the presence of KF had a relatively low rate at room temperature, this reaction was also investigated at higher temperatures, and the results are shown in Figure 5. It can be seen that the temperature does not significantly influence the reaction rate in the temperature range from 22 to 60 °C. The experimental data were fitted to eq 3, giving values of the apparent rate constant k of 1.0, 1.3, and 3.6 mol^{-1} h^{-1} for the reaction at 22, 40, and 60 °C, respectively. From these data it can be seen that increasing the reaction temperature from 22 to 60 °C results in only a 3-fold increase in reaction rate. This result indicates that the reaction is also influenced by a process with a low activation energy. Following the above discussion, the apparent rate constant $k = Kk_p[K^+]/[HF]$. Traditionally, it is believed that the solid KF in the solution acts as a KF reservoir to keep $[K^+]$ constant in the solution during a reaction. However, as the molecular weight gets higher, the polymer will adsorb on the solid surface, acting as a barrier layer to reduce the diffusion of KF from solid into the solution. This will result in an low value of $[K^+]$ in the solution. Therefore, KF diffusion might become an important factor in controlling the reaction rate. We believe that it is these diffusion-controlled kinetics that subsequently lead to a low-temperature dependence of the reaction rate.

6. Thermal Properties of the Polymers. The thermal properties of the produced polymers have been analyzed by DSC and TGA. Figure 6 displays DSC curves from the second heating scan of these polymers. These curves indicate that the T_gs of the polymers gradually decrease from 102.6 to 78.3 °C as the length of the fluorinated aliphatic spacers increases from 4 to 10 carbons. This behavior is similar to that of analogous polyesters with hydrogenous aliphatic spacers,[14] suggesting a

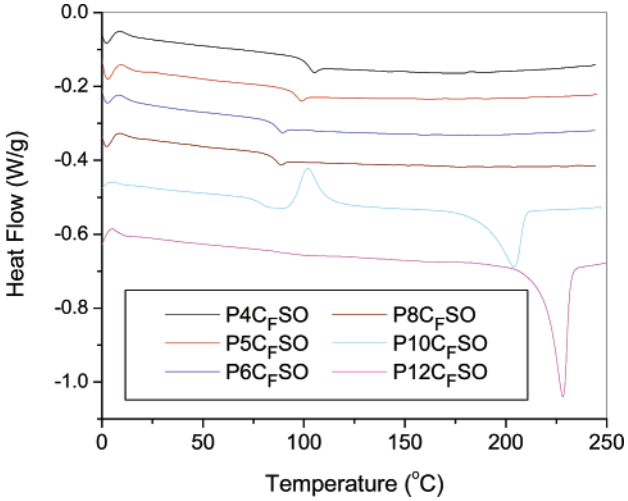

Figure 6. DSC curves of the second heating scan of PmC$_F$SO. Samples were cooled from 250 °C at 10 °C/min. P10C$_F$SO and P12C$_F$SO were quenched from 250 °C using liquid nitrogen.

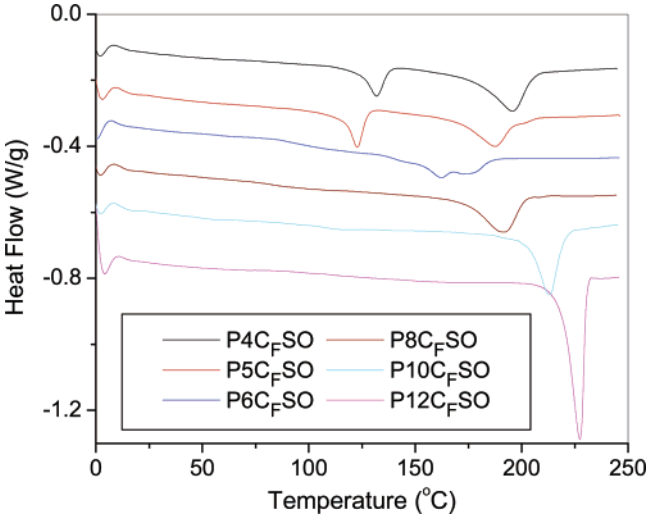

Figure 7. DSC curves of first heating scan of the as-prepared PmC$_F$SO samples.

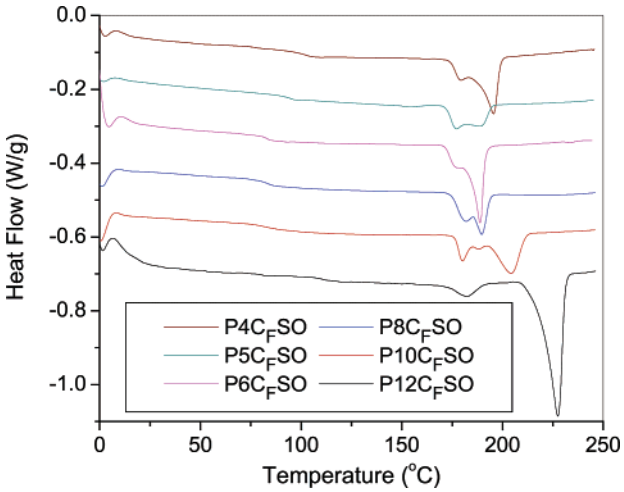

Figure 8. DSC curves of the annealed PmC$_F$SO samples (at 165 °C for 14 h).

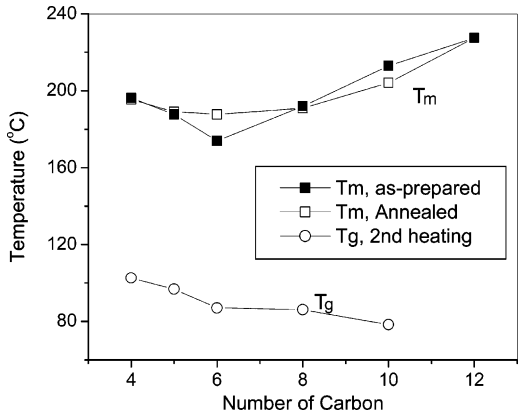

Figure 9. Variation of the T_m and T_g values of PmC$_F$SO samples as a function of the number of carbon atoms in the fluorinated alkylene spacers.

similar behavior in contributing to chain flexibility of both fluorinated and hydrogenous aliphatic spacers. The fluorine atom has a much larger volume than hydrogen, and the polarity of the C−F bond is much higher than that of the C−H bond. These factors are both expected to produce higher steric hindrance and cause a higher rigidity of the polymer chain with a longer fluorinated alkylene spacer. However, the low polarizability[1a] of the fluorine atom and the highly symmetric structure of the fluorinated alkylene spacer result in lower intermolecular forces in the fluorinated chain than in the hydrogenous analogues. The combination of these effects results in an increased flexibility of the polymer with the increased length of the fluorinated alkylene spacers. This feature also leads to low surface energies and low refractive indices of the highly fluorinated polymers.[1a]

While a well-defined glass transition was observed from the second scan curves of the polymers with a shorter alkylene spacer containing 4−8 carbons, only a melting peak but no glass transition was observed for the polymers with longer alkylene spacers (P10C$_F$SO and P12C$_F$SO). These two polymers were reanalyzed by DSC using quenched samples (by immersing the molten sample at 250 °C into liquid nitrogen). P10C$_F$SO displayed a well-resolved glass transition at 78.3 °C, followed by a fast crystallization peak at 101.9 °C. The heat (exothermic) of this peak is 8.86 J/g, about 65% of the endothermic of the melting peak at 204.2 °C (13.69 J/g). This data implies that the sample partially crystallized during the quenching process, indicating a high crystallization rate for this polymer. This conclusion is supported by the DSC analysis of the quenched sample of P12C$_F$SO, in which only a strong melting peak was observed at 227 °C, with no observable glass transition. This result suggests that P12C$_F$SO crystallized completely during the quenching process, indicating an extremely high crystallization rate for this polymer.

In addition to the strong crystallization tendency of P10C$_F$SO and P12C$_F$SO, all the other polymers with linear aliphatic spacers showed some crystallization capabilities as depicted in Figure 7, where the first heating scans of the as-prepared samples are displayed. From this figure a broad primary melting peak is observed for all of the polymers with linear spacers. The values of T_m and ΔH of these polymers are summarized in Table 1, which indicates that P6C$_F$SO had the lowest T_m and ΔH values among all of the polymers with linear alkylene spacers. In order to eliminate the effect of thermal history on this melting behavior, the as-prepared samples were also annealed at 165 °C for 14 h and then evaluated by DSC with the results shown in Figure 8. The variation of the T_m and T_g as a function of the number of carbon atoms in the fluorinated alkylene spacers is summarized in Figure 9. Once again, P6C$_F$SO shows the lowest T_m. This phenomenon is different from that of the analogous nonfluorinated polyesters,[14] for which T_m decreased from 340 to 230 °C as the length of the aliphatic spacer increased from 2 to 10 carbons, in addition to an odd−even effect of the carbon

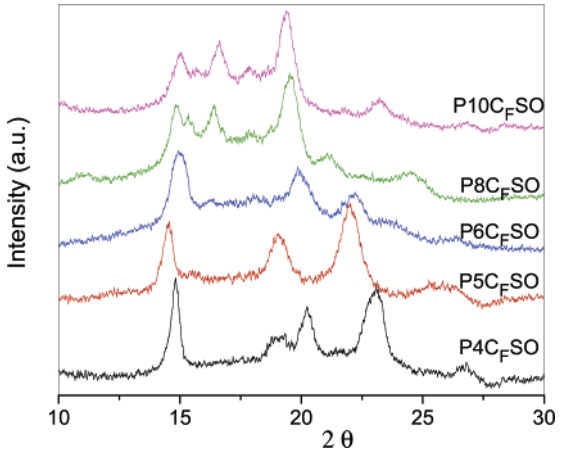

Figure 10. XRD profiles of the as-prepared PmC$_F$SO samples.

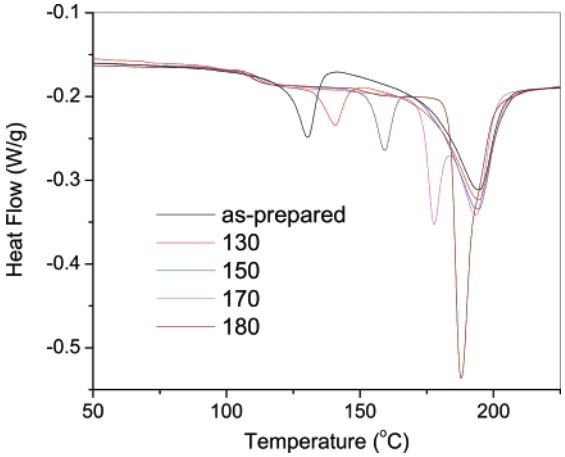

Figure 11. DSC curves of P4C$_F$SO samples which were annealed at 130, 150, 170, or 180 °C for 30 min.

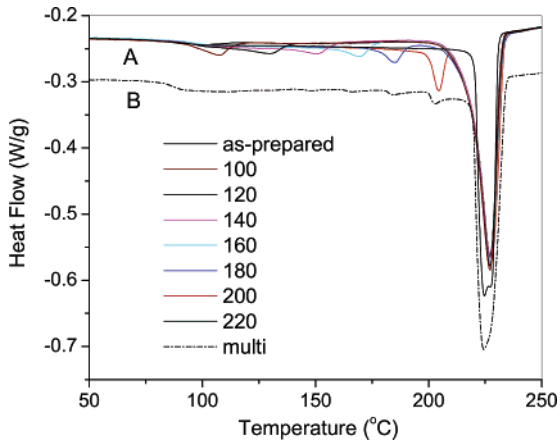

Figure 12. Effect of annealing on the DSC curves of the quenched P12C$_F$SO samples (from 250 °C into liquid nitrogen). (A) The samples were annealed at 100, 120, 140, 160, 180, 200, and 220 °C for 30 min. (B) The sample was annealed by a step sequence involving successively holding at 220, 200, 180, 160, 140, 120, and 100 °C for 30 min for each step.

number on the T_m associated with hydrogen bonding. Since there is no hydrogen-bonding interaction in our polymer system, it is easy to understand why no odd−even effect was found. However, it is challenging to understand why T_m of the polymers in this study initially decreases with the length of alkylene spacers and then increases when the spacer is longer than 6 carbons.

It should be noted that the structure of the fluorinated aliphatic spacers corresponds closely to poly(tetrafluoroethylene), a highly crystalline polymer with a T_m of 332 °C and ΔH of 82.0 J/g.[15] If all of the polymers with different length of aliphatic spacers possess a similar crystallization capability and form a similar type of crystals, the T_m values of these polymers should monotonically increase from 196.2 °C for P4C$_F$SO to 332 °C for the polymer with an infinite length of the aliphatic spacer. The observation of the lowest T_m for P6C$_F$SO may indicate that the type of crystal formed in the polymers with alkylene spacer shorter than six carbons is different from that longer than six carbons. This assumption has been confirmed by X-ray diffraction (XRD) study of the as-prepared samples with the results presented in Figure 10. It can be seen that P10C$_F$SO, P8C$_F$SO, and P6C$_F$SO all have very similar diffraction patterns, which are significantly different from the patterns from P5C$_F$SO and P4C$_F$SO.

7. Secondary Crystal Peak. The DSC curves shown in Figure 7 also indicated a secondary melting peak at 132.0 and 122.5 °C for P4C$_F$SO and P5C$_F$SO, respectively. In order to investigate the origin of this peak, as-prepared samples of P4C$_F$SO were annealed at different temperatures in the region between the secondary melting peak and the primary melting peak for 30 min, and then a DSC measurement was performed with the results shown in Figure 11. It can be seen that the annealing moved the second melting peak toward a temperature about 8−10 °C higher than the annealing temperature with a slightly increased intensity. At the same time, the annealing process did not apparently influence the intensity and the position of the primary melting peak. This result indicates that this secondary melting peak corresponds to a secondary crystal structure, which is not able to be converted to the primary crystal before the primary crystal melts. Similar phenomena have been also found in some other types of polymers such as polyesters.[16]

To better understand this phenomenon, the annealing effect was also investigated on the quenched sample of P12C$_F$SO, which did not show any secondary melting peak originally. In this case, the quenched samples were annealed for 30 min at different temperatures between 100 and 220 °C, 7 °C below the melting point of the primary crystal. The results are presented in Figure 12A. Interestingly, even though no secondary melting peak is observed from the parent sample (the quenched sample) as shown in Figure 6, a secondary melting peak was observed in all of the annealed samples, with the peak position about 5−10 °C higher than the annealing temperature. This feature is very similar to that of P4C$_F$SO. However, annealing P4C$_F$SO moved the secondary melting peak to a higher temperature, while annealing P12C$_F$SO produced a secondary melting peak. In both cases, the annealing did not affect the primary crystal peak. Even when the sample was annealed at 220 °C, only 7 °C lower than the primary crystal peak, the position of the primary peak remained unchanged, although some overlap with the secondary peak with a maximum at 224 °C did occur. This result indicated that the secondary melting peak can be created during annealing. However, the structure related to this secondary peak will not convert to the primary crystal, as long as the primary crystal is not melted. In order to exclude the possibility that the secondary peak is just a simple memory of the annealing history but not related to any morphological structure, the quenched P12C$_F$SO sample was also annealed using an annealing sequence, in which the sample was heated successively at 220, 200, 180, 160, 140, 120, and 100 °C for 30 min at each step. The DSC trace of this sample is displayed in Figure 12B. It can be seen that, after this annealing sequence, only a few weak secondary melting peaks can be identified corresponding to the annealing steps at high temperatures (220, 200, and 180

°C). This indicated that the secondary melting peak is related to morphological structures consisting of a certain number of chain segments. Once this form of the material has formed a type of secondary crystal at a higher temperature, it will not be converted by annealing at a lower temperature. This material in the original quenched sample should be in an amorphous state. However, no corresponding glass transition was found from the quenched sample, as shown in Figure 7. A similar phenomenon has also been reported for some other polymers, and the corresponding material was referred to as "rigid amorphous",[16d,e] where the chain segments have very low mobility. This is associated with the very limited size, location, and occupied space of these chain segments which are restricted by the primary crystal structures. On the basis of all this knowledge, we can conclude that the secondary crystal is a type of incomplete crystallite formed between the sheets of primary lamellar crystals. The limited chain mobility and chain length of these chain segments and the available space restricted by the primary crystals prevented these secondary crystals from maturing into primary crystals. On the other hand, because of the limited mobility of these chain segments, these secondary crystals only formed at lower rates, and therefore none of these structures are formed during the quenching process, even for the highly crystalline P12C_FSO.

Conclusion

Highly fluorinated poly(arylene akylene ether sulfone)s have been prepared from nucleophilic polycondensation reactions of DPSO with a series of linear or branched fluorinated alkylene diols containing 4−12 carbons. The reactions are activated using CsF or KF as a base in DMAc. CsF exhibits a high activity, allowing the reaction to complete in a few hours at room temperature. In comparison, the activity of KF is relatively low and the required reaction time at room temperature is on the order of a few days. Increasing the reaction temperature does not significantly enhance the reaction rate. Because of low solubility, CsF and KF exist in the reaction solution mainly in the form of solid particles. The resulting polymer tends to adsorb on the surface of the particles, forming a barrier layer and preventing the diffusion of CsF or KF from the solid into solution. As a result, the base concentration near the solid surface is much higher than in solution, resulting in a higher polymerization rate and thus higher molecular weight polymers in the region close to the particle surface than in solution. The final polymer thus exhibits a broad molecular weight distribution. On the other hand, the presence of this barrier layer slows down the supply of the base into the solution, and as a result the diffusion of the base has a great effect on the reaction kinetics, leading to a low-temperature dependence of the reaction rate. High molecular weight polymers have been obtained from all of the fluorinated diols, except the one with longest alkylene spacer (12C_F-diol). This polymer exhibits a very strong tendency to crystallize and crystallized during the polymerization. The formation of crystals prevented further growth of the polymer chains at 22 and 40 °C. Increasing the reaction temperature to 70 °C slightly retards the crystallization, and a polymer with a M_n of 17 700 Da is obtained. All of the polymers with linear alkylene spacers show some tendency to crystallize, while the polymer from the branched diol (P7$_b$$C_F$SO) is completely amorphous. As the length of the linear alkylene spacer increases from 4 to 6 carbons, the melting temperature of the polymers decreases. However, further increasing the alkylene spacer length to 12 carbons yields an increase of the melting temperature. This finding suggests that different types of crystals are formed for polymers with alkylene spacer shorter than and those longer than six carbons. All of the crystalline polymers display a secondary melting peak in the DSC curves. On annealing, the position of this peak shifts to a temperature about 5−10 °C higher than the annealing temperature. However, this peak never merges into the primary melting peak as long as the primary crystal is not melted. The secondary melting peak is attributed to the chain segments located between the sheets of the primary lamellae. The limited size, mobility, and restricted space of these chain segments which are confined by the lamellae structures of the primary crystals prevent them from maturing to the primary crystal form.

Experimental Section

Materials. Fluorinated alkylene diols including 1*H*,1*H*,4*H*,4*H*-perfluoro-1,4-butanediol (4C_F-diol), 1*H*,1*H*,5*H*,5*H*-perfluoro-1,5-pentanediol (5C_F-diol), 1*H*,1*H*,6*H*,6*H*-perfluoro-1,6-hexanediol (6C_F-diol), 1*H*,1*H*,8*H*,8*H*-perfluoro-1,8-octanediol (8C_F-diol), 1*H*,1*H*,-10*H*,10*H*-perfluoro-1,10-decanediol (10C_F-diol), 1*H*,1*H*,12*H*,12*H*-perfluoro-1,12-dodecanediol (12C_F-diol), and 2-fluoro-2-perfluorobutyl-1,3-propanediol (7$_b$$C_F$-diol) were purchased from Oakwood Products Inc. and used as received. Decafluorodiphenyl sulfone (DPSO) was prepared according to a reported method.[6f] All other chemicals were purchased from Sigma-Aldrich and used as received.

Characterizations. Nuclear magnetic resonance (NMR) spectra were recorded using a Varian Unity Inova spectrometer at a resonance frequency of 400 MHz for ^{1}H NMR and 376 MHz for ^{19}F NMR in acetone-d_6. The solutions taken from the reaction at different reaction times were directly used for kinetics study, while purified polymers were used for structural analysis. The chemical shifts relative to tetramethylsilane for ^{1}H NMR and $CFCl_3$ for ^{19}F NMR are reported on the ppm scale. The molecular weights of the polymers were determined by size exclusion chromatography (SEC) using a Viscotek SEC system, which consists of a Viscotek VE1122 HPLC pump coupled with a Viscotek TDA triple detector and a Viscotek 2501 UV detector operated at 260 nm. A set of ViscoGEL columns (G4000H and G5000H) was used and calibrated using a set of polystyrene standards in THF. The MALDI-TOF mass spectra were done on a Voyager-DE STR MALDI-TOF (Applied Biosystems, Foster City, CA) operated in the reflection positive mode. Samples dissolved in THF were spotted using dithranol matrix in chloroform/acetone (1:1, v/v). IR spectra were recorded with a Midac M1200-SP3 spectrophotometer from film samples for polymers, and a diamond cell was used for powder samples. Differential scanning calorimetric (DSC) measurements and thermogravimetric analyses (TGA) were performed on a TA Instruments DSC 2920 and on a TA Instruments TGA 2950, respectively, using a heating rate of 10 °C/min under nitrogen.

Synthesis of P6C_FSO from DPSO and 6C_F-diol in the Presence of KF. To a solution of DPSO (1.6013 g, 4.02 mmol) and 6C_F-diol (1.048 g, 4.00 mmol) in anhydrous DMAc (16 mL) was added KF (0.697 g, 12.0 mmol). The mixture was vigorously stirred at room temperature. 0.2 mL aliquots of the reaction solution were removed at desired times for NMR and GPC analysis. The solution was filtered through a cotton plug in a pipet to remove solids; 0.05 mL of the filtrate was dropped into 0.5 mL of acetone-d_6 for ^{19}F NMR analysis, and the rest of the filtrate was dropped into a methanol/H_2O (50/50) mixture to precipitate the polymer and oligomers for SEC analysis. After reacting for 150 h, the solution was centrifuged to remove inorganic salts and then added dropwise into HCl/methanol (0.5 mL/200 mL) with stirring. The resulting fibrous white polymer was collected by filtration, washed thoroughly with water and methanol, and dried at room temperature under vacuum for 12 h. ^{1}H NMR (400 MHz, acetone-d_6), δ (ppm): 5.19 (m). ^{19}F NMR (376 MHz, acetone-d_6), δ (ppm): −121.84 (4F, m), −124.31 (4F, m), −140.0 (4F, m), −155.79 (4F, m). IR (film, cm^{-1}): 2982 (CH stretching), 1638, 1500 (phenyl ring), 1177, 1128 (ether), 1013, 990, 583, 559. T_g: 88.2 °C. T_m: 168.3 and 177.7 °C. M_n: 30 600 Da. M_w/M_n: 4.6.

Synthesis of P6C$_F$SO from DPSO and 6C$_F$-diol in the Presence of CsF. To a solution of DPSO (1.6013 g, 4.02 mmol) and 6C$_F$-diol (1.048 g, 4.00 mmol) in anhydrous DMAc (16 mL) was added CsF (1.922 g, 12.0 mmol). The mixture was stirred at room temperature for 4.0 h. After centrifuging to remove inorganic salts, the polymer solution was added dropwise into HCl/methanol (0.5 mL/200 mL) with stirring. The resulting fibrous white polymer was collected by filtration, washed thoroughly with water and methanol, and dried at room temperature under vacuum for 12 h (2.23 g, 90% yield). ^{1}H NMR (400 MHz, acetone-d_6), δ (ppm): 5.20 (m). ^{19}F NMR (376 MHz, acetone-d_6), δ (ppm): −121.86 (4F, m), −124.33 (4F, m), −139.88 (4F, m), −155.81 (4F, m). T_g: 87.0 °C. T_m: 162.1, and 173.9 °C. M_n: 44 000 Da. M_w/M_n: 6.5.

Synthesis of the Other Polymers. The other polymers were prepared from the corresponding diols using the same procedure as described above with the reaction time listed in Table 1 and characterized as follows:

P4C$_F$SO (80% yield). ^{1}H NMR (400 MHz, acetone-d_6), δ (ppm): 5.14 (t). ^{19}F NMR (376 MHz, acetone-d_6), δ (ppm): −123.68 (4F), −139.98 (4F), −155.96 (4F). IR (film, cm^{-1}): 2982 (CH stretching): 1638, 1498 (phenyl ring), 1180, 1125 (ether), 997, 596, 559. T_g: 102.6 °C. T_m: 196.2 °C. M_n: 41 500 Da. M_w/M_n: 4.5.

P5C$_F$SO (86% yield). ^{1}H NMR (400 MHz, acetone-d_6), δ (ppm): 5.17 (t). ^{19}F NMR (376 MHz, acetone-d_6), δ (ppm): −122.09 (4F), −126.12 (2F), −139.91 (4F), −155.85 (4F). IR (film, cm^{-1}): 2981 (CH stretching), 1637, 1498 (phenyl ring), 1170, 1127 (ether), 1021, 990, 583, 559. T_g: 96.8 °C. T_m: 187.7 °C. M_n: 41 000 Da. M_w/M_n: 4.9.

P8C$_F$SO (85% yield). ^{1}H NMR (400 MHz, acetone-d_6), δ (ppm): 5.24 (t). ^{19}F NMR (376 MHz, acetone-d_6), δ (ppm): −121.64 (4F), −123.01 (4F), −124.01 (4F), −139.87 (4F), −155.80 (4F). IR (film, cm^{-1}): 2981 (CH stretching), 1636, 1500 (phenyl ring), 1201, 1176, 1134 (ether), 1021, 990, 581, 558. T_g: 86.1 °C. T_m: 192.0 °C. M_n: 85 300 Da. M_w/M_n: 6.0.

P10C$_F$SO (82% yield). ^{1}H NMR (400 MHz, acetone-d_6), δ (ppm): 5.26 (t). ^{19}F NMR (376 MHz, acetone-d_6), δ (ppm): −121.6 (4F), −122.82 (8F), −123.92 (4F), −139.88 (4F), −155.81 (4F). IR (film, cm^{-1}): 2981 (CH stretching), 1638, 1500 (phenyl ring), 1210, 1175, 1146 (ether), 990, 584, 558. T_g: 78.3 °C. T_m: 213.0 °C M_n: 33 000 Da. M_w/M_n: 3.8.

P7$_b$C$_F$SO (83% yield). ^{1}H NMR (400 MHz, acetone-d_6), δ (ppm): 5.17 (m). ^{19}F NMR (376 MHz, acetone-d_6), δ (ppm): −82.19 (3F), −119.87 (2F), −122.76 (2F), −126.92 (2F), −139.96 (4F), −155.85 (4F), −183.62 (1F). IR (diamond cell, cm^{-1}): 2982 (CH stretching), 1638, 1504 (phenyl ring), 1387, 1237, 1179, 1139 (ether); 1010, 587, 559. T_g: 94.7 °C. M_n: 12 200 Da. M_w/M_n: 3.4.

Synthesis of P12C$_F$SO from DPSO and 12C$_F$-diol in the Presence of CsF/CaH$_2$. To a solution of DPSO (0.8044 g, 2.02 mmol) and 6C$_F$-diol (1.1249 g, 2.00 mmol) in anhydrous DMAc (12 mL) was added CsF, (0.152 g, 1.0 mmol) and CaH_2 (0.168 g, 4.0 mmol). The mixture was stirred at 70 °C, and 8 mL of DMAc was added in 2 h. The reaction was finished in 5.0 h, and the microgel-like polymer solution was added dropwise into 400 mL of methanol/H_2O (50/50) mixture with stirring. The resulting white powder was collected by filtration, washed thoroughly with acidic water and methanol, and dried at room temperature under vacuum for 12 h (2.18 g, 88% yield). ^{1}H NMR (400 MHz, acetone-d_6), δ (ppm): 5.26 (t). ^{19}F NMR (376 MHz, acetone-d_6), δ (ppm): −121.65 (4F), −122.85 (12F), −124.05 (4F)−140.0 (4F), −156.05 (4F). IR (diamond cell, cm^{-1}); 2981 (CH stretching), 1638, 1498 (phenyl ring), 1290, 1207, 1130 (ether), 1000, 650, 558. T_m: 227.5 °C. M_n: 17 700 Da. M_w/M_n: 3.1.

Acknowledgment. J.D. thanks Dr. Jacques Roovers for fruitful discussions.

References and Notes

(1) For example, see review articles: (a) Grainger, D. W.; Stewart, C. W. In *Fluorinated Surfaces, Coatings and Films*; Castner, D. G., Grainger, D. W., Eds.; American Chemical Society: Washington, DC, 2001; pp 1−14. (b) Souzy, R.; Ameduri, B. *Prog. Polym. Sci*. **2005**, *30*, 644−687. (c) Hickner, M. A.; Ghassemi, H.; Kim, Y. S.; Einsla, B. R.; McGrath, J. E. *Chem. Rev.* **2004**, *104*, 4587−4612. (d) Zhou, M. *Opt. Eng.* **2002**, *47*, 1631−1643.

(2) Johncock, P.; Hewins, M. A. H.; Cunliffe, A. V. *J. Polym. Sci., Polym. Chem*. **1976**, *14*, 365−378.

(3) Feiring, A. E.; Wondhoba, E. R. *J. Polym. Sci., Part A: Polym. Chem.* **1994**, *32*, 389−392.

(4) Miyatake, K.; Oyaizu, K.; Tsuchida, E.; Hay, A. *Macromolecules* **2001**, *34*, 2065−2071.

(5) Kim, T. K.; Kim, J. H. U.S. Patent, US2002/0057882-A2.

(6) (a) Ding, J.; Day, M. *Macromolecules* **2006**, *39*, 6054−6062. (b) Qi, Y.; Ding, J.; Day, M.; Jiang, J.; Callender, C. L. *Chem. Mater*. **2005**, *17*, 676−682. (c) Ding, J.; Qi, Y.; Day, M.; Jiang, J.; Callender, C. L. *Macromol. Chem. Phys.* **2005**, *206*, 2396−2400. (d) Ding, J.; Day, M.; Robertson, G. P.; Roovers, J. *Macromol. Chem. Phys.* **2004**, *205*, 1070−1079. (e) Ding, J.; Liu, F.; Li, M.; Day, M.; Zhou, M. *J. Polym. Sci., Part A: Polym. Chem.* **2002**, *40*, 4205−4216. (f) Liu, F.; Ding, J.; Li, M.; Day, M.; Robertson, G.; Zhou, M. *Macromol. Rapid Commun.* **2002**, *23*, 844−848.

(7) Attwood, T. E.; Barr, D. A.; King, T.; Newton, A. B.; Rose, J. B. *Polymer* **1977**, *18*, 359−364.

(8) Imai, Y.; Yamanaka, K.; Ishikawa, H.; Kakimoto, M. *Macromol. Chem. Phys.* **1999**, *200*, 95−99.

(9) Imai, Y.; Ishikawa, H.; Park, K.-H.; Kakimoto, M.-A. *J. Polym. Sci., Part A: Polym. Chem.* **1997**, *35*, 2055−206.

(10) Elias, H.-G. In *Macromolecules 2, Synthesis and Materials*; Stafford, J. W., Translator; Plenum Press: New York, 1977; p 599.

(11) Smith, M. B.; March, J. *March's Advanced Organic Chemistry*, 5th ed.; John Wiley & Sons: New York, 2001; p 850.

(12) (a) Kricheldorf, H. R.; Vakhtangishvili, L.; Schwarz, G.; Schulz, G.; Krüger, R.-P. *Polymer* **2003**, *44*, 4471−4480. (b) Kricheldorf, H. R.; Schwarz, G. *Macromol. Rapid Commun.* **2003**, *24*, 359−381. (c) Kricheldorf, H. R.; Böhme, S.; Schwarz, G.; Krüger, R.-P.; Schulz, G. *Macromolecules* **2001**, *34*, 8886−8893. (d) Colquhoun, H. M.; Lewis, D. F.; Hodge, P.; Ben-Haida, A.; Williams, D. J.; Baxter, I. *Macromolecules* **2002**, *35*, 6875−6882.

(13) (a) Goodwin, A. A.; Mercer, F. W.; McKenzie, M. T. *Macromolecules* **1997**, *30*, 2767−2774. (b) Kimura, K.; Tabuchi, Y.; Yamashita, Y.; Cassidy, P. E.; Fitch, J. W., III; Okumura, Y. *Polym. Adv. Technol*. **2000**, *11*, 757−765. (c) Lee, H.-J.; Lee, M.-H.; Oh, M.-C.; Ahn, J.-H.; Han, S. G. *J. Polym. Sci., Part A: Polym. Chem.* **1999**, *37*, 2355−2361.

(14) Goodman, I. In *Encyclopedia of Polymer Science and Engineering*; Kroschwitz, J., Ed.; John Wiley and Sons: New York, 1990; Vol. 12, p 10.

(15) Van Krevelen, D. W. *Properties of Polymers*, 3rd ed.; Elsevier Science: New York, 1990; p 790.

(16) (a) Yagphanov, M. *J. Therm. Anal.* **1986**, *31*, 1073−1082. (b) Kriegel, R. M.; Collard, D. M.; Liotta, C. L.; Schiraldi, D. A. *Macromol. Chem. Phys.* **2001**, *202*, 1776−1781. (c) Roupakias, C. P.; Papageorgiou, G. Z.; Karayannidis, G. P. *J. Macromol. Sci., Pure Appl. Chem.* **2003**, *40*, 791−805. (d) Kampert, W. G.; Sauer, B. B. *Polymer* **2000**, *42*, 8703−8714. (e) Sauer, B. B.; Kampert, W. G.; Mclean, R. S.; Carcia, P. F. *J. Therm. Anal. Calorim.* **2000**, *59*, 227−243.

MA070013Y